Methods 49 (2009) 189–196

Contents lists available at ScienceDirect

Methods

journal homepage: www.elsevier.com/locate/ymeth

The jerky and knotty dynamics of RNA

Hervé Isambert

RNA Dynamics and Biomolecular Systems, Institut Curie, Centre de Recherche, CNRS UMR168, 11, rue P.&M. Curie, 75005 Paris, France

ARTICLE INFO

Article history:
Accepted 19 June 2009
Available online 27 June 2009

Keywords:
RNA folding dynamics
Pseudoknot
Entanglement
RNA simulation
RNA self-assembly
Non-coding RNA

ABSTRACT

RNA is known to exhibit a jerky dynamics, as intramolecular thermal motion, on <0.1 μs time scales, is punctuated by infrequent structural rearrangements on much longer time scales, *i.e.* from >10 μs up to a few minutes or even hours. These rare stochastic events correspond to the formation or dissociation of entire stems through cooperative base pairing/unpairing transitions. Such a clear separation of time scales in RNA dynamics has made it possible to implement coarse grained RNA simulations, which predict RNA folding and unfolding pathways including kinetically trapped structures on biologically relevant time scales of seconds to minutes. RNA folding simulations also enable to predict the formation of pseudoknots, that is, helices interior to loops, which mechanically restrain the relative orientations of other non-nested helices. But beyond static structural constraints, pseudoknots can also strongly affect the folding and unfolding dynamics of RNA, as the order by which successive helices are formed and dissociated can lead to topologically blocked transition intermediates. The resulting knotty dynamics can enhance the stability of RNA switches, improve the efficacy of co-transcriptional folding pathways and lead to unusual self-assembly properties of RNA.

1. Introduction

RNA folding dynamics and folding pathways have long been suspected to play an active role in helping proper native folding of ribozymes and structured regulatory motifs in mRNA untranslated regions (UTRs) [1].

Indeed, because of their limited four-letter alphabet and strong base pair stacking energies, RNAs are prone to adopt long-lived misfolded structures [2], as observed for instance upon heat renaturation. Hence, efficient RNA folding paths leading to properly folded structures bear an important role in the regulatory function of non-coding RNAs and mRNA untranslated regions (UTRs) [1].

I review in this paper, some of the specificities of RNA folding dynamics, in particular, the *jerky* and sometime *knotty* dynamics of RNA folding/unfolding transitions. These unique features and their implications for RNA dynamics are illustrated with some of our recent numerical and experimental studies on synthetic or natural non-coding RNAs.

2. Jerky dynamics of cooperative base pairing/unpairing

RNA exhibits a jerky dynamics punctuated by the formation or dissociation of entire helices through cooperative base pairing/unpairing transitions [3,4], Fig. 1. These large but infrequent structural rearrangements occur on >10 μs time scales that are much longer than intramolecular thermal motion (zipping/unzipping base pairs and backbone conformational changes) occurring on <0.1 μs time scales. Yet, the formation of new helices remains much faster (10–100 μs) than the time needed to synthesize a full transcript, resulting into co-transcriptional folding pathways for 0.1 s up to a few minutes depending on transcript length and RNA polymerase. But the eventual relaxation of new transcripts into their equilibrium structures might take much longer, *e.g.* minutes to hours or even days (that is, longer than the typical timespan of RNA before degradation in the cell, *i.e.* 1 min to 1 h).

2.1. RNA folding is slow compared to intramolecular motion

The clear separation of time scales between the folding dynamics of nucleic acid (>10 μs) and the rapid intramolecular thermal motion (<0.1 μs) and heat diffusion at these scales ($<10^{-3}$ μs for a heat diffusion coefficient of about 10^{-7} m^2/s) can be directly used to control the folded state of nanomolecular switches through rapid cooling steps (>100 °C/ms) [5].

The same separation of time scales has also been used to develop coarse grained dynamics simulations, which predict RNA folding pathways including kinetically trapped structures on biologically relevant time scales of seconds to minutes [6–9]. Simulated folding paths then correspond to discrete series of secondary structures related through successive additions or removals of single helices, Fig. 2.

Yet, for the same reason that actual RNA molecules are prone to remained trapped in metastable structures, it happens frequently

E-mail address: herve.isambert@curie.fr

1046-2023/$ - see front matter © 2009 Elsevier Inc. All rights reserved.
doi:10.1016/j.ymeth.2009.06.005

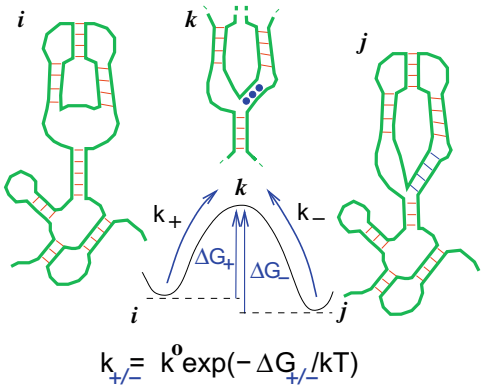

Fig. 1. RNA dynamics involves cooperative base pairing or unpairing transitions between RNA structures [3,4]. These time limiting steps of RNA folding/ unfolding dynamics can be modelled by Arrhenius rates, corresponding to rare escapes across transition barriers, on >10 μs up to minute or hour time scales, compared to the much faster intramolecular thermal motion (zipping/unzipping base pairs and backbone conformational changes) on <0.1 μs time scales.

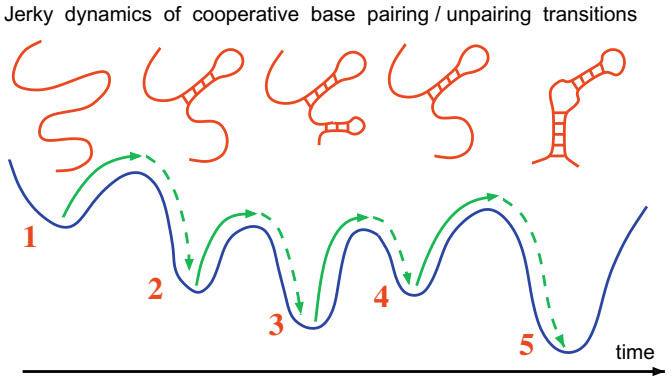

Fig. 2. RNA dynamics simulations follow the stochastic formation and removal of individual helices, which are known to be the time limiting steps of RNA/DNA folding kinetics from seminal experimental results [3,4]. The time step increment, corresponding to the average delay until the next Arrhenius transition (Fig. 1), reads $\tau_i = \Sigma_i k_i^{-1}$, where $k_i = k^\circ \exp - \Delta G_i/kT$ [6,7,9] (Fig. 1).

that simulated trajectories oscillate repeatedly between a few structures, and only much more slowly transit to visit new configurations. To circumvent these local kinetic traps which can severely impact the efficiency of the code, we have developed and implemented [8,9] 'exactly clustered stochastic simulations' which continuously averaged folding paths at the level of rapidly exchanging structures (see details in Ref. [8]).

Hence, simulations of RNA folding paths [6–14], which provide unique insights into RNA folding traps, can usefully complement the predictions of RNA minimum free energy structures, traditionally done with efficient 'dynamic programming' algorithms [15–20].

In particular, RNA folding simulations can investigate co-transcriptional pathways [7,9,21], that is, the folding of nascent RNA transcripts while their sequence is still being transcribed.

2.2. RNA folding is fast compared to transcription rate

The reason why nascent RNA transcripts actually fold during transcription is that the folding dynamics of new RNA hairpins occurs on 10–100 μs time scales, which, although molecularly slow (see above), remains much faster than the time needed to synthesize a full transcript, *i.e.* 1 s to 1 min for a 300 nucleotides (nt) transcript depending on the RNA polymerase used (bacteriophage 3 ms/nt; bacteria 20 ms/nt; eukaryote 200 ms/nt).

In fact, it has long been proposed [22–24] that, during transcription, the progressive folding of nascent RNAs limits the number of folding pathways, presumably facilitating their rapid folding into proper native structures.

The importance of co-transcriptional folding pathways has subsequently been demonstrated in a series of inspiring studies [11,25–30,13,31–36]. In particular, the efficacy of RNA folding pathways has been shown to depend on the type of RNA polymerase used, as well as on the conditions of transcription, such as temperature and NTP concentrations, which all affect the average transcription rate [37]. In addition, specific pause sites along co-transcriptional folding pathways were also shown to ensure proper sequential folding into independent RNA domains [31].

More recently, we have however shown experimentally [21] that folded domains do not simply fold sequentially and independently from one another during transcription. Instead, efficient folding paths actually result from intricate interactions between helices susceptible to form at successive steps of transcription, as early simulations already suggested [7]. In particular, we could demonstrate, using sequence symmetries of bistable RNA switches [21], that folding paths can be essentially decoupled from equilibrium structures, Fig. 3.

Hence, native and transiently formed helices can efficiently guide co-transcriptional folding of RNA switches into different alternative long-lived structures. Such folding path is controlled by the order of helix nucleations and subsequent exchanges during transcription, and may also be redirected by transient antisense interactions, Fig. 3.

2.3. RNA relaxation is slow compared to mechanical unfolding

Yet, co-transcriptionally folded RNAs might not have relaxed into their minimum free energy structures by the end of transcription. This is because RNAs are proned to remain trapped in suboptimum structures for minutes to hours or even days.

This slow relaxation dynamics has been directly observed under micromechanical unfolding experiments of single RNA molecules, which probe both their native and long-lived intermediate structures [38].

In particular, micromechanical stretching of the 1540-nt 16S ribosomal RNA of *Escherichia coli* was found to result in a surprisingly well-structured and reproducible unfolding pathway, which could be compared to out-of-equilibrium stochastic unfolding simulations, Fig. 4 [38].

This example illustrates what should be expected, in general, when large RNA secondary structures are probed by mechanical force. Strong helices resist until their breaking exposes weaker regions, which are unable to withstand the same high force. This leads to the unfolding of a significant domain with a concomitant force drop. A fraction of the unpaired bases then typically reform different helices, which compensate, in part, for the sudden relaxation of the mechanical tension. Yet, force-extension responses are not completely smoothed out, as would be expected for long RNA sequences (>1000 nt) unfolding under quasistatic equilibrium. This reveals the slow dynamics of large scale cooperative changes in large RNA structures.

3. RNA pseudoknots create RNA knots

Another unique feature of RNA folding simulations is their ability to include and effectively predict the formation of "pseudoknots" [7–10]. Pseudoknots (Fig. 5) are helices interior to loops which constrain the end-to-end distance of the single strands

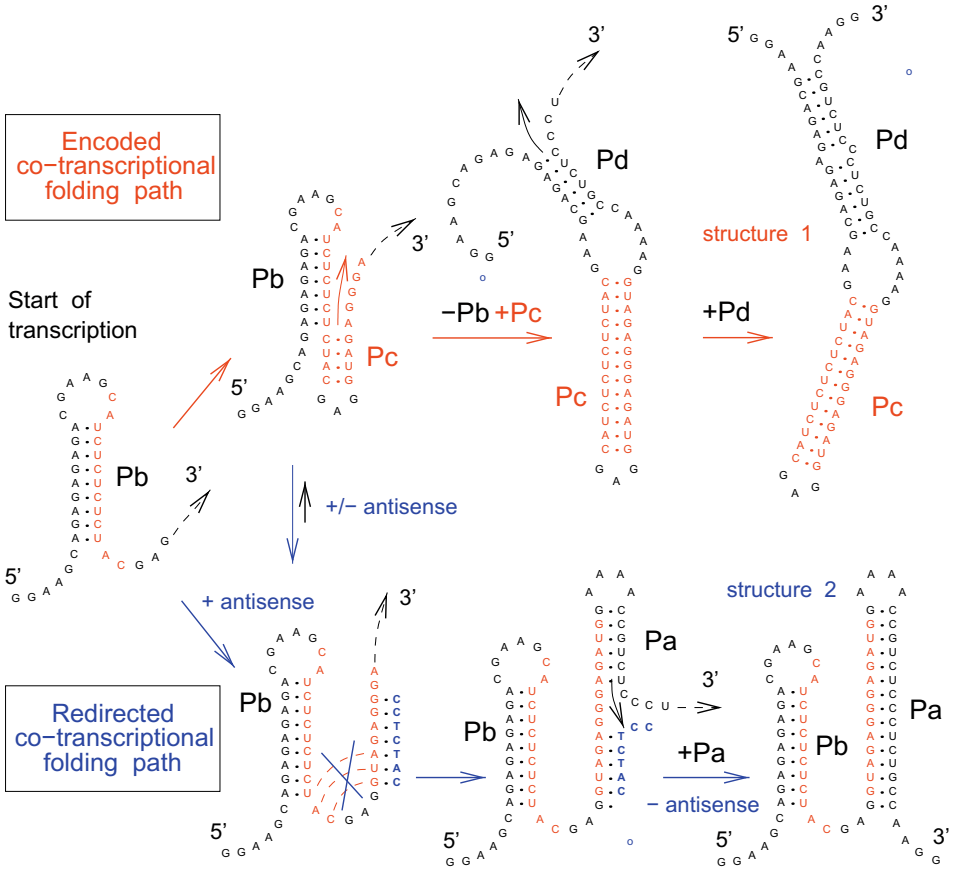

Fig. 3. Encoded co-transcriptional folding path (top) and its redirection through transient antisense interaction (bottom) of a bistable RNA switch [21]. Co-transcriptional folding is biased towards one structure which can remain out-of-equilibrium for several hours at 37 °C, whereas the RNA transcripts eventually partition about equally between the two structures at equilibrium.

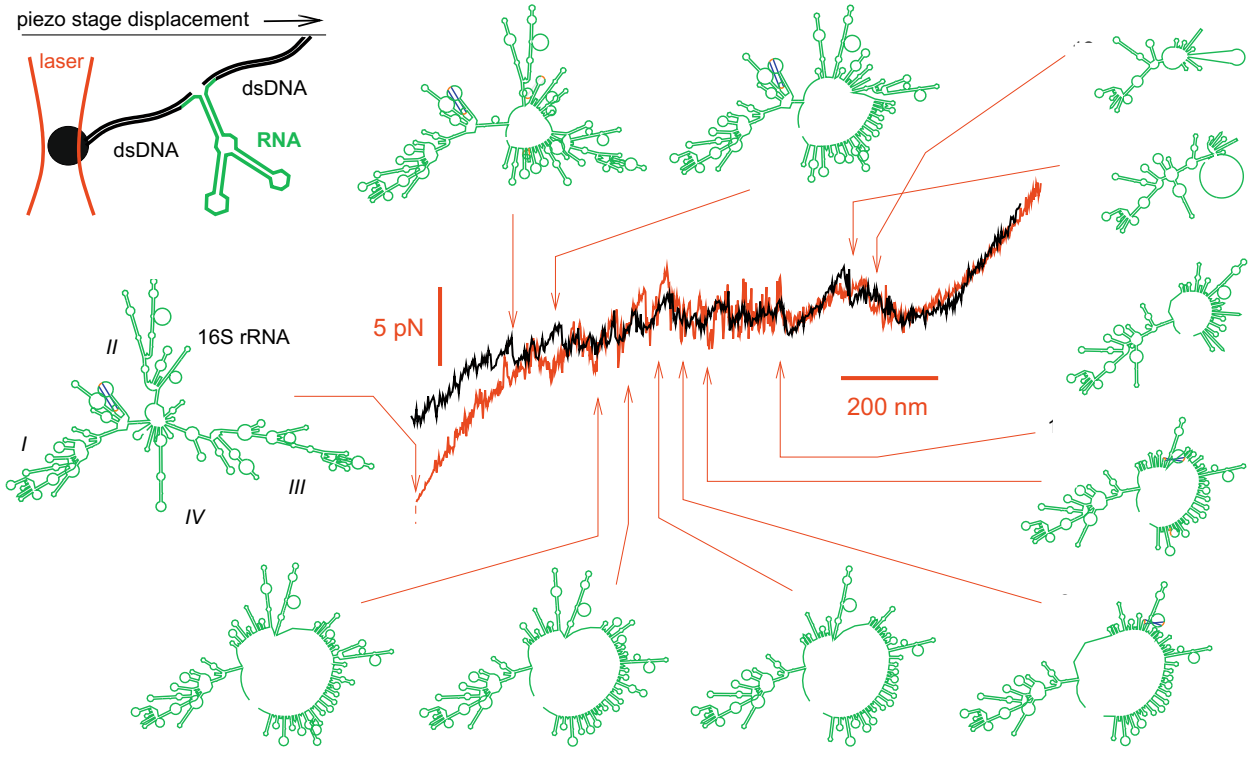

Fig. 4. Comparison between simulated force-extension response from the known native structure (red) and an experimental stretching curve (black) of the 1540-nt 16S ribosomal RNA of *E. coli* [38]. Stretching-induced intermediates, predicted from the simulated unfolding pathway(red), are drawn starting with the known native structure of 16S rRNA. Single stranded regions under tension are not drawn for convenience, hence the overall decreasing size of the structure under stretching.

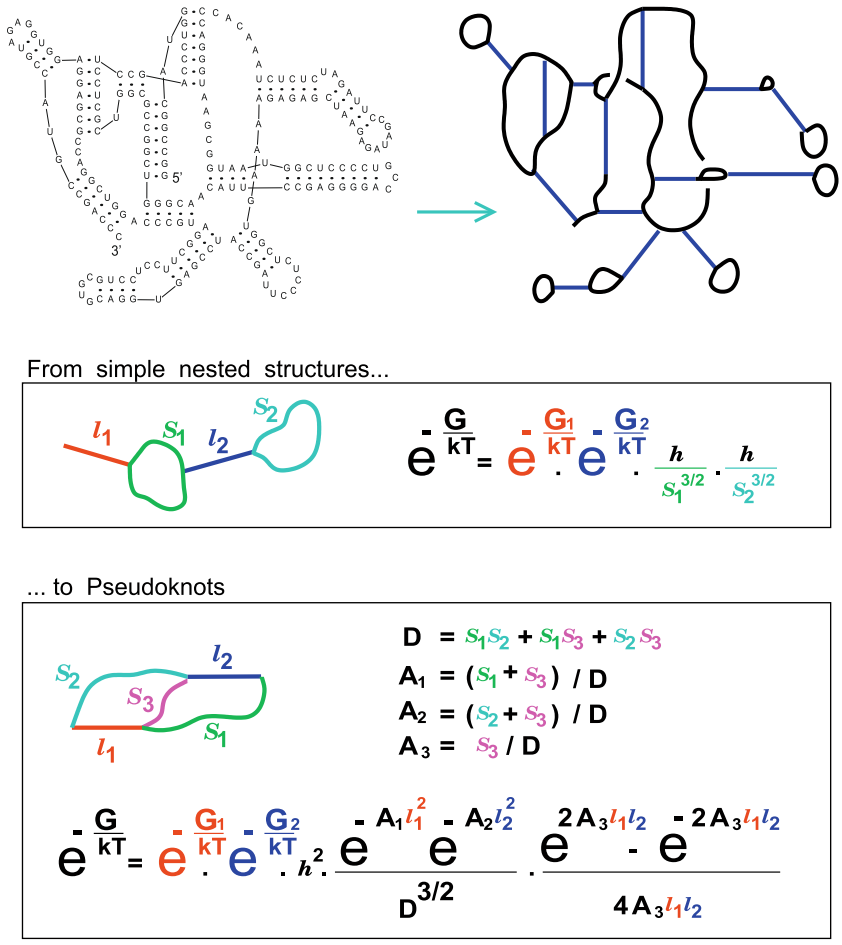

Fig. 5. RNA structures including pseudoknots can be modeled as mixed assemblies of ideal polymer springs (corresponding to single strands) linking stiff rods (corresponding to individual stems of the RNA structure). This allows to estimate the free energy contribution of pseudoknots in RNA structures and evaluate free energy barriers to model and simulate RNA folding dynamics including pseudoknots [7–9].

bridging their extremities and the global orientation of other non-nested helices, Fig. 5. Owing to their non-nested character, pseudoknot helices are difficult to predict through traditional free energy minimization schemes using "dynamic programming" algorithms [39–44], which are more adapted to hierarchical tree-like structures.

But beyond folding dynamics *vs.* free energy minimization approaches, the prediction of pseudoknots requires an estimate of their contribution to global free energy of RNA structures.

The 3D *static* constraints caused by pseudoknots have been estimated using polymer physics approaches of increasing complexity, from simple loop parameters [45–47] to more detailed structural features, combining single-stranded with double-stranded regions [7,9,48–50]. In particular, the entropic stretching of single strands and the global correlation between helix orientations have been evaluated by modeling RNA helices as stiff rods and single-stranded regions as polymer springs, Fig. 5.

But beyond these static structural constraints, which mechanically restrain the relative orientations of other helices, pseudoknots can also strongly affect the folding *dynamics* of RNA. This is because the order by which successive helices are formed and dissociated in an RNA structure can lead to topologically blocked, or *knotted*, transition intermediates [9], Fig. 6.

In other words, pseudoknots, which are not themselves entangled, do nonetheless create topological entanglements, or *knots*, in RNA structures. Yet, the entanglement of a 'knotted' helix does *not* require that one single strand is threaded through a loop of the RNA structure, as might be expected at first sight to make a knot. Instead, knotted helices are simply trapped by their own helicity and a nearby pseudoknot, provided that they are longer than about half a helix turn (>6 bp). In that case, their *dissociation* becomes topologically impeded by the presence of the pseudoknot, as their unpaired strands cannot freely separate due to the residual "tangle" (after Conway's classification of knots [51]) left behind by the unpaired helix. Such a knotted helix generally cannot be dissociated until *all* pseudoknots blocking its release by free rotation are *simultaneously* removed. This significantly increases kinetic dissociation barriers of unfolding Arrhenius transition, hence, effectively leaving knotted helices kinetically trapped.

4. Knotty dynamics of topologically blocked transitions

The existence of knotted intermediates in RNA folding/unfolding pathways results in a *knotty* dynamics that can enhance the stability of RNA switches [9], improve the efficacy of co-transcriptional folding pathways [52] and lead to unusual self-assembly properties of RNA [53].

4.1. Blocked transitions in RNA co-transcriptional folding

In co-transcriptional folding paths, topologically blocked transition intermediates typically arise when the position of an early

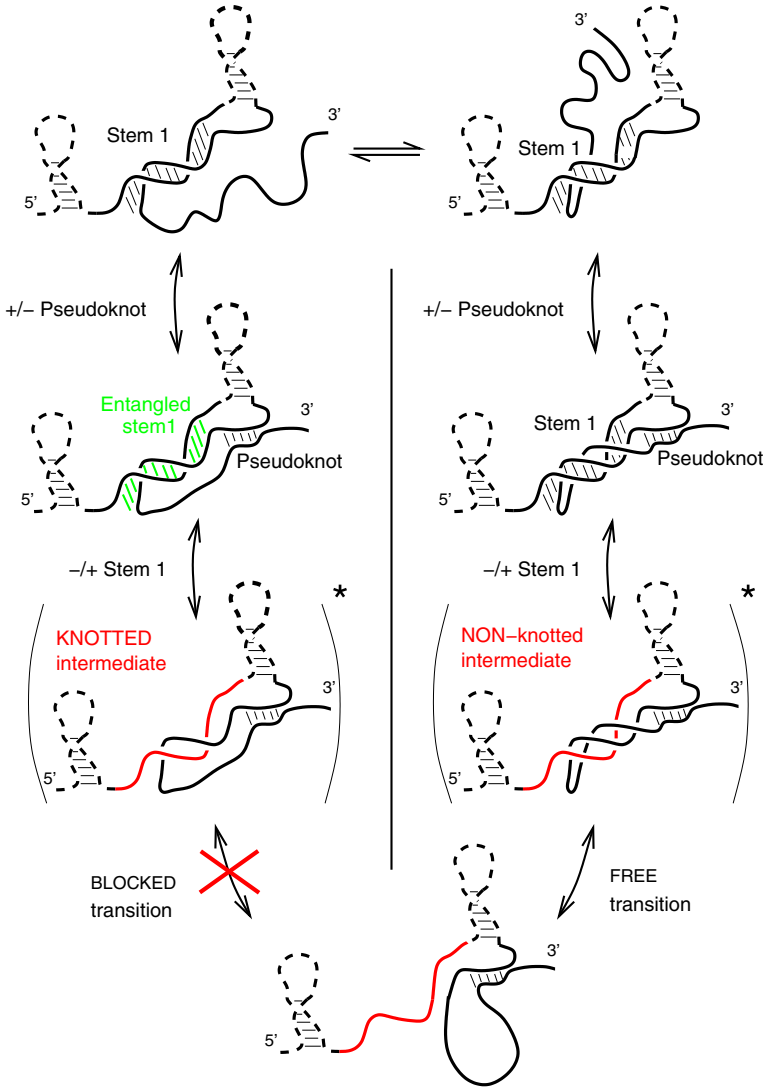

Fig. 6. Entangled helices, or RNA *knots* arise because the order by which successive helices are formed and dissociated can lead to topologically blocked transition intermediates [9]. RNA knots are simply trapped by their own helicity and a nearby pseudoknot, provided that they are longer than about half a helix turn (>6 bp). In that case, their *dissociation* becomes topologically impeded by the presence of the pseudoknot.

folded stem overlaps with the loop region of a second helix, encoded downstream along the sequence, Fig. 7. This favors the nucleation of the second helix by its base rather than its loop, leading to a kotted intermediate that blocks subsequent exchange of stability between the two helices.

Topologically blocked intermediates may cause, in particular, long-lived metastable structures of UTR RNA switches regulating the expression of downstream genes at the level of either transcription (*e.g.* control of early termination/antitermination) or translation (*e.g.* control of Shine-Dalgarno motif sequestration). Such RNA switches can also be controlled through antisense RNA–RNA interaction, as in the case of tRNA-mediated transcription antitermination in *Bacillus subtilis* and other Gram-positive bacteria [54,55]. Synthetic ribozymes activated via antisense interactions have also been successfully designed [56].

More recently, we also demonstrated through synthetic biology design guided by advanced RNA simulations that RNA can also perform elementary regulation tasks [52]. We have shown, in particular, that RNA synthetic regulatory modules directly inspired from bacterial transcription attenuators can efficiently activate or repress the expression of other RNAs by merely controlling their folding paths 'on the fly' during transcription through simple RNA–RNA antisense interaction [52].

From an 'RNA world' perspective, this suggests that direct coupling between synthesis, folding and regulation of RNAs may have indeed enabled the early emergence of autonomous RNA-based regulation networks in the absence of both DNA and protein partners.

4.2. Blocked transitions can promote RNA self-assembly

While multimeric proteins as well as larger protein self-assemblies such as in the cytoskeleton are relatively common, natural RNA tend to remain monomeric. This is in fact all the more surprising, as many large artificial nanostructures made of DNA [57–71] or RNA [72–75] have been successfully designed, using Watson–Crick pairing rules or tertiary RNA–RNA motif interactions. But these artificial nanostructures are implemented through highly

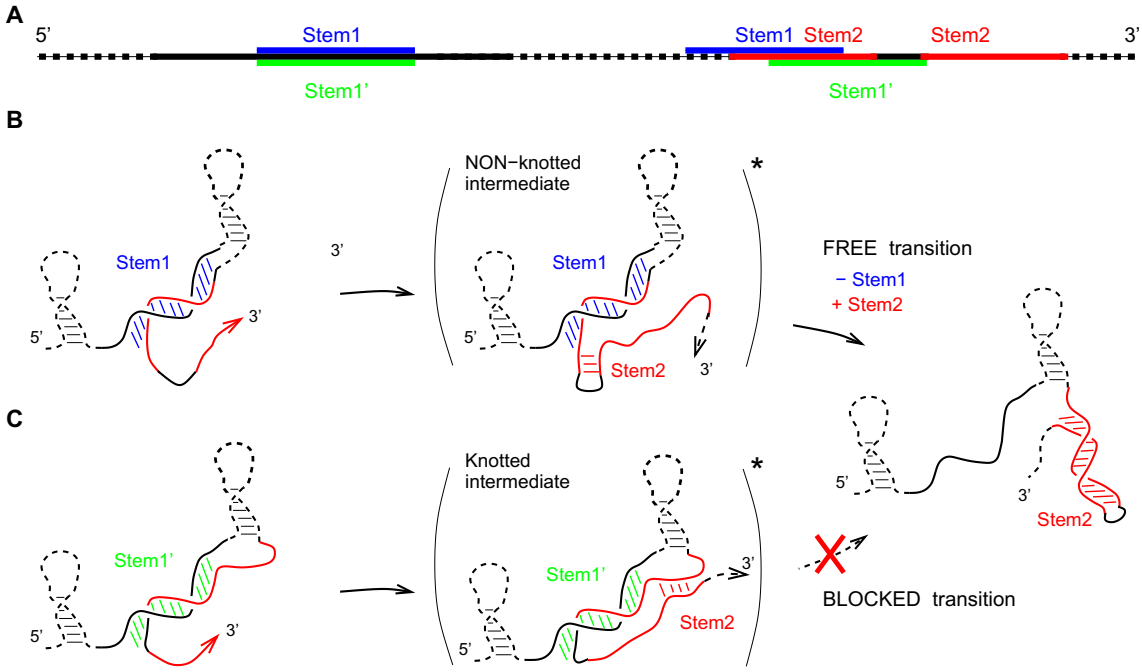

Fig. 7. (A) Efficient co-transcriptional folding paths rely on the precise positional order of helices along the 5′ to −3′ oriented sequence as well as the relative stability between successive helices. (B) If the position of first folded Stem1 does not overlap with the loop region of Stem2, it enables the nucleation of stem2 by its loop and subsequent exchange of stability between the two helices through branch migration process. (C) By contrast, if the position of first folded Stem1' overlaps with the loop region of Stem2, it favors the nucleation of stem2 by its base rather than its loop, leading to a kotted intermediate that blocks subsequent exchange of stability between the two helices.

constraining sequence heuristics that prevent the formation of alternative intramolecular pairings in place of the designed intermolecular interactions. Typical heuristics are based on the limitation of short complementary substring occurrences in the sequence [76,77].

By contrast, natural RNA sequences, that are presumably void of such strong sequence constraints, are expected to favor intramolecular base pairing instead of intermolecular interactions, thanks to their overall flexibility, Fig. 8A.

Yet, we have recently shown, that topological barriers might actually prevent the simultaneous formation of non-overlapping helices within monomeric or dimeric RNA structures [53]. Topologically blocked intramolecular transitions might then favor intermolecular interactions (Fig. 8A) that lead to the formation of extended self-assemblies of bacterial non-coding RNA [53], Fig. 8B.

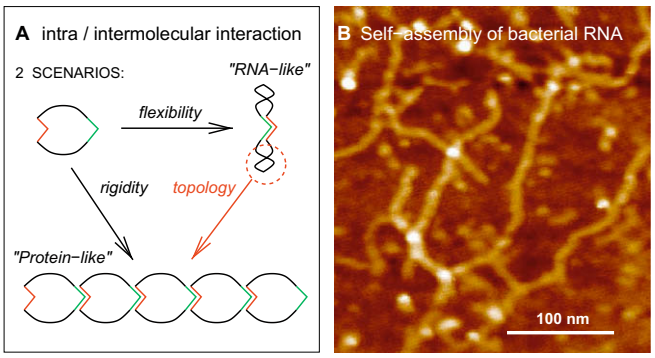

Fig. 8. (A) Topologically blocked intramolecular transitions in RNA can favor intermolecular interactions and lead to the formation of extended RNA self-assemblies, as typically observed with proteins. (B) Self-assembly of a non-coding RNA of *Escherichia coli*, observed by atomic force microscopy [53].

5. Kinefold server: online RNA/DNA folding simulations

The theoretical and experimental results reviewed in this paper have been predicted, analyzed or designed with advanced stochastic RNA folding/unfolding simulations. Most of them have been performed online using the Kinefold RNA/DNA folding simulation server [9], which can be accessed at http://kinefold.curie.fr/.

The Kinefold web server provides a web interface for stochastic folding simulations of nucleic acids on second to minute molecular time scales. It proposes two folding dynamics scenarios: 'renaturation' or 'co-transcriptional folding' pathways, which are simulated at the level of helix formation and dissociation in agreement with seminal experimental results on the separation of time scales for RNA dynamics [3,4] (see above). Further information on the available simulation options and algorithmic features are provided in [9] and [8].

Pseudoknots and topologically 'entangled' helices (*i.e.* RNA knots) are efficiently predicted taking into account simple geometrical and topological constraints, as outline above. See also [7–9] for further technical aspects.

To encourage interactivity, simulations launched as immediate jobs are automatically stopped after a few seconds and return adapted recommendations. Users can then choose to continue incomplete simulations using the batch queuing system or go back and modify suggested options in their initial query.

The detailed output of Kinefold provides: (1) a series of low free energy structures, (2) an online animated folding path and (3) a programmable trajectory plot focussing on a few helices of interest to each user, Fig. 9. See [9] for detailed descriptions of output files and formats.

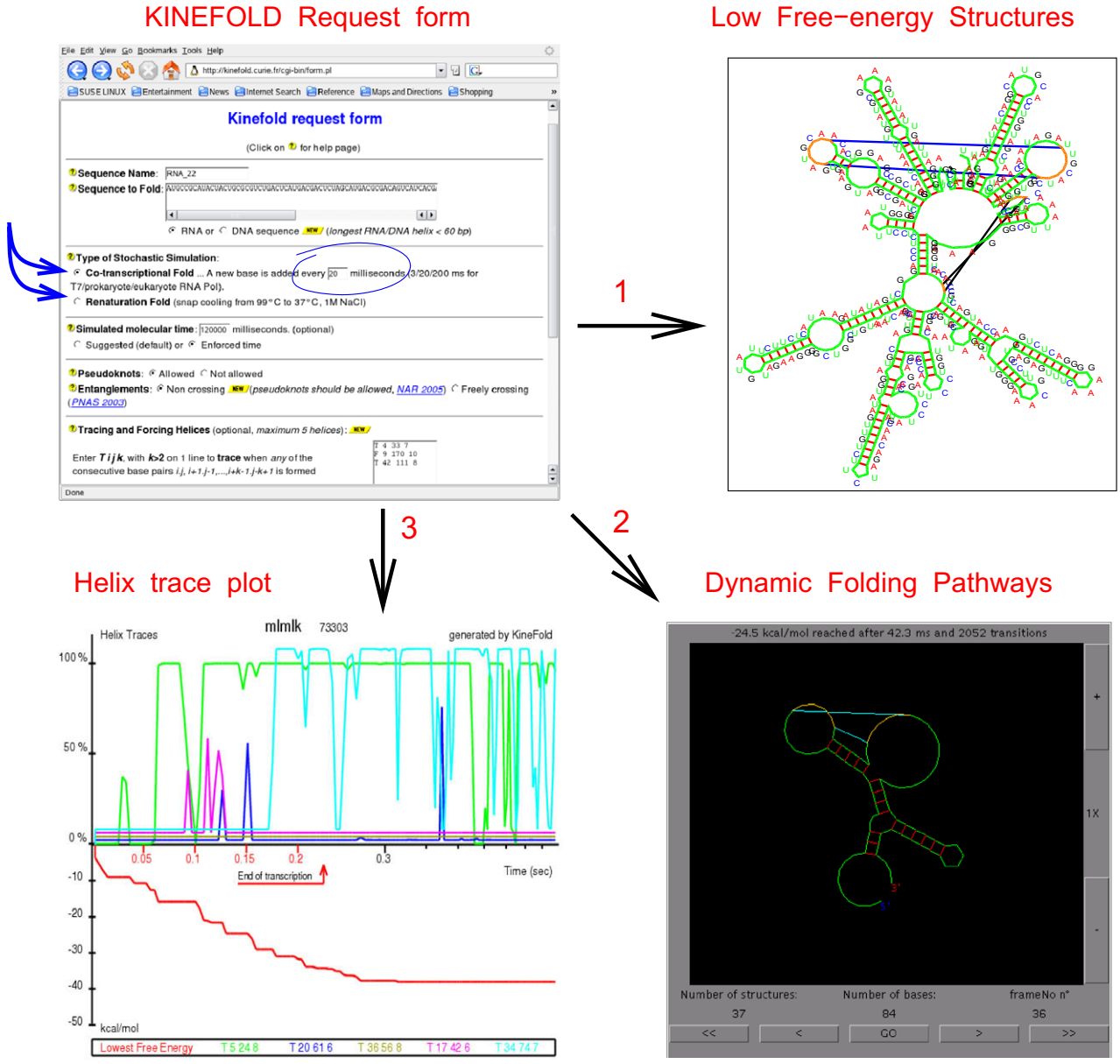

Fig. 9. Kinefold request form and detailed output providing (1) a series of low free energy structures, (2) an online animated folding path and (3) a programmable trajectory plot focussing on a few helices of interest to each user [9].

Acknowledgements

I am grateful to T. Buchert, B. Cayrol, D. Chatenay, A. Dawid, S. Harlepp, A. Meller, C. Nogues, J. Robert, I. Sagi, E.D. Siggia, P. Silberzan, F. Thalmann, V. Viasnoff, and A. Xayaphoummine for their contributions to the projects illustrating this review. I am also grateful for stimulating discussions and interactions with D. Evers, C. Flamm, L. Jaeger, I. Hofacker, L. Hirschbein, E. Heard, C. Lemoine, C.W. Pleij, H. Putzer, N. Seeman, M. Springer, H. Touzet about these studies. This work was supported in part by HFSP Grant RGP0036/2005C, ANR PNANO Grant 015-03, Institut Curie and CNRS.

References

[1] O.C. Uhlenbeck, RNA 1 (1995) 4–6.
[2] S. Morgan, P.J. Higgs, Chem. Phys. 105 (1996) 7152–7157.
[3] M.E. Craig, D.M. Crothers, P.J. Doty, Mol. Biol. 62 (1971) 383–401.
[4] D. Pörschke, Biophys. Chem. 1 (1974) 381–386.
[5] V. Viasnoff, A. Meller, H. Isambert, Nano Lett. 6 (2006) 101–104.
[6] A.A. Mironov, L.P. Dyakonova, A.E.J. Kister, Biomol. Struct. Dynam. 2 (1985) 953–962.
[7] H. Isambert, E.D. Siggia, Proc. Natl. Acad. Sci. USA 97 (2000) 6515.
[8] A. Xayaphoummine, T. Bucher, F. Thalmann, H. Isambert, Proc. Natl. Acad. Sci. USA 100 (2003) 15310–15315.
[9] A. Xayaphoummine, T. Bucher, H. Isambert, Nucleic Acids Res. 33 (2005) 605–610.
[10] A.P. Gultyaev, Nucleic Acids Res. 19 (1991) 2489–2494.
[11] A.P. Gultyaev, F.H. van Batenburg, C.W. Pleij, Nucleic Acids Res. 23 (1995) 3718–3725.
[12] A.P. Gultyaev, F.H. van Batenburg, C.W.J. Pleij, Mol. Biol. 276 (1998) 43–55.
[13] J.H. Nagel, A.P. Gultyaev, K. Gerdes, C.W. Pleij, RNA 5 (1999) 1408–1418.
[14] C. Flamm, W. Fontana, I.L. Hofacker, P. Schuster, RNA 6 (2000) 325–338.
[15] M.S. Waterman, T.F. Smith, Math. Biosci. 42 (1978) 257–266.
[16] R. Nussinov, G. Pieczenik, J.R. Griggs, D.J. Kleitman, SIAM J. Appl. Math. 35 (1978) 68–82.
[17] R. Nussinov, A.B. Jacobson, Proc. Natl. Acad. Sci. USA 77 (1980) 7826–7830.
[18] M. Zuker, P. Stiegler, Nucleic Acids Res. 9 (1981) 133–148.
[19] J.S. McCaskill, Biopolymers 29 (1990) 1105–1119.
[20] I.L. Hofacker, W. Fontana, P.F. Stadler, L.S. Bonhoeffer, M. Tacker, P. Schuster, Monatsh. Chem. 125 (1994) 167–188.

[21] A. Xayaphoummine, V. Viasnoff, S. Harlepp, H. Isambert, Nucleic Acids Res. 35 (2007) 614622.
[22] J. Boyle, G. Robillard, S.J. Kim, Mol. Biol. 139 (1980) 601–625.
[23] F. Kramer, D. Mills, Nucleic Acids Res. 9 (1981) 5109–5124.
[24] R. Nussinov, I. Tinoco Jr., J. Mol. Biol. 151 (1981) 519–533.
[25] H. Groeneveld, K. Thimon, J. van Duin, RNA 1 (1995) 79–88.
[26] R.A. Poot, N.V. Tsareva, I.V. Boni, J. van Duin, Proc. Natl. Acad. Sci. USA 94 (1997) 10110–10115.
[27] K. Gerdes, A.P. Gultyaev, T. Franch, K. Pedersen, N.D. Mikkelsen, Annu. Rev. Genet. 31 (1997) 1–31. review.
[28] A.P. Gultyaev, T. Franch, K.J. Gerdes, Mol. Biol. 273 (1997) 26–37.
[29] T. Franch, A.P. Gultyaev, K.J. Gerdes, Mol. Biol. 273 (1997) 38–51.
[30] D. Repsilber, S. Wiese, M. Rachen, A. Schroder, D. Riesner, G. Steger, RNA 5 (1999) 574–584.
[31] T. Pan, I. Artsimovitch, X. Fang, R. Landick, T.R. Sosnick, Proc. Natl. Acad. Sci. USA 96 (1999) 9545–9550.
[32] S.L. Heilman-Miller, S.A. Woodson, RNA 9 (2003) 722–733.
[33] S.P. Koduvayur, S.A. Woodson, RNA 10 (2004) 1526–1532.
[34] J.K. Wickiser, W.C. Winkler, R.R. Breaker, D.M. Crothers, Mol. Cell 18 (2005) 49–60.
[35] E.M. Mahen, J.W. Harger, E.M. Calderon, M.J. Fedor, Mol. Cell 19 (2005) 27–37.
[36] Tao Pan, Tobin Sosnick, Annu. Rev. Biophys. Biomol. Struct. 35 (2006) 161–175.
[37] M. Chamberlin, J. Ring, J. Biol. Chem. 248 (1973) 2235–2244.
[38] S. Harlepp, T. Marchal, J. Robert, J.-F. Léger, A. Xayaphoummine, H. Isambert, D. Chatenay, Eur. Phys. J. E12 (2003) 605–615.
[39] J.P. Abrahams, M. van den Berg, E. van Batenburg, C.W.A. Pleij, Nucleic Acids Res. 18 (1990) 3035–3044.
[40] E. Rivas, S.R. Eddy, J. Mol. Biol. 285 (1999) 2053–2068.
[41] T. Akutsu, Discrete Appl. Math. 104 (2000) 45–62.
[42] R. Lyngsø, C.J. Pedersen, Comput. Biol. 7 (2000) 409–427.
[43] R. Dirks, N.A. Pierce, J. Comput. Chem. 24 (2003) 1664.
[44] J. Ruan, G. Stormo, W. Zhang, Bioinformatics 20 (2004) 58–66.
[45] H.M. Martinez, Methods Enzymol./ 183 (1990) 306–318.
[46] A.A. Mironov, V.F. Lebedev, BioSystems 30 (1993) 4956.
[47] A.P. Gultyaev, E. van Batenburg, C.W.A. Pleij, RNA 5 (1999) 60961.
[48] D.P. Aalberts, N.O. Hodos, Nucleic Acids Res. 33 (2005) 2210–2214.
[49] S. Cao, S.-J. Chen, Nucleic Acids Res. 34 (2006) 2634–2652.
[50] W.K. Dawson, K. Fujiwara, G. Kawai, PLoS ONE 2 (2007) e905.
[51] J.H. Conway, in: J. Leech (Ed.), Computation Problems in Abstract Algebra, Pergamon Press, Oxford, 1967, pp. 329–358.
[52] A. Dawid, B. Cayrol, H. Isambert, RNA synthetic biology inspired from bacteria: construction of transcription attenuators under antisense regulation, Phys. Biol. 6 (2) (2009) 25007.
[53] B. Cayrol, C. Nogues, A. Dawid, I. Sagi, P. Silberzan, H. Isambert, A novel nanostructure made of bacterial non-coding RNA, submitted for publication.
[54] H. Putzer, C. Condon, D. Brechemier-Baey, R. Brito, M. Grunberg-Manago, Transfer RNA-mediated antitermination in vitro, Nucleic Acids Res. 30 (2002) 3026–3033.
[55] F.J. Grundy, W.C. Winkler, T.M. Henkin, Proc. Natl. Acad. Sci. USA 99 (2002) 11121–11126.
[56] R. Penchovsky, R.R. Breaker, Nat. Biotechnol. 23 (2005) 1424–1433.
[57] X. Yang, L.A. Wenzler, J. Qi, X. Li, N.C. Seeman, J. Am. Chem. Soc. 120 (1998) 9779–9786.
[58] E. Winfree, F. Liu, L.A. Wenzler, N.C. Seeman, Nature 394 (1998) 539–544.
[59] C. Mao, W. sun, N.C. Seeman, J. Am. Chem. Soc. 121 (1999) 5437–5443.
[60] L. Feng, S.H. Park, J.H. Reif, H. Yan, Angew. Chem. Int. Ed. Engl. 42 (2003) 4342–4346.
[61] P.W.K. Rothemund et al., J. Am. Chem. Soc. 126 (2004) 16344–16352.
[62] P.W.K. Rothemund, N. Papadakis, E. Winfree, PLoS Biol. 2 (2004) e424.
[63] N. Chelyapov et al., J. Am. Chem. Soc. 126 (2004) 13924–13925.
[64] B. Ding, R. Sha, N.C. Seeman, J. Am. Chem. Soc. 126 (2004) 10230–10231.
[65] W.M. Shih, J.D. Quispe, G.F. Joyce, Nature 427 (2004) 618–621.
[66] H. Liu, Y. Chen, Y. He, A.E. Ribbe, C. Mao, Angew. Chem. Int. Ed. Engl. 45 (2006) 1942–1945.
[67] B. Ding, N.C. Seeman, Science 314 (2006) 1583–1585.
[68] R. Schulman, E. Winfree, Proc. Natl. Acad. Sci. USA 104 (2007) 15236–15241.
[69] Y. He et al., Nature 452 (2008) 198–201.
[70] P. Yin, H.M.T. Choi, C.R. Calvert, N.A. Pierce, Nature 451 (2008) 318–322.
[71] P. Yin et al., Science 321 (2008) 824–826.
[72] L. Jaeger, N.B. Leontis, Angew. Chem. Int. Ed. Engl. 39 (2000) 2521–2524.
[73] A. Chworos et al., Science 306 (2004) 2068–2072.
[74] D. Shu, W.-D. Moll, Z. Deng, C. Mao, P. Guo, Nano Lett. 4 (2004) 1717–1723.
[75] L. Nasalean, S. Baudrey, N.B. Leontis, L. Jaeger, Nucleic Acids Res. 34 (2006) 1381–1392.
[76] N.C. Seeman, J. Theor. Biol. 99 (1982) 237–247.
[77] R.M. Dirks, M. Lin, E. Winfree, N.A. Pierce, Nucleic Acids Res. 32 (2004) 1392–1403.